PHYSICAL REVIEW D **76,** 044008 (2007)

Consistency of $f(R) = \sqrt{R^2 - R_0^2}$ gravity with cosmological observations in the Palatini formalism

M. Sadegh Movahed,[1,2] Shant Baghram,[3] and Sohrab Rahvar[3]

[1]*Department of Physics, Shahid Beheshti University, Evin, Tehran 19839, Iran*
[2]*Institute for Studies in Theoretical Physics and Mathematics, P.O. Box 19395-5531, Tehran, Iran*
[3]*Department of Physics, Sharif University of Technology, P.O. Box 11365-9161, Tehran, Iran*

(Received 7 May 2007; revised manuscript received 16 June 2007; published 8 August 2007)

In this work we study the dynamics of the Universe in $f(R) = \sqrt{R^2 - R_0^2}$ modified gravity with the Palatini formalism. We use data from recent observations, such as the supernova type Ia Gold sample and Supernova Legacy Survey data, the size of the baryonic acoustic peak from the Sloan Digital Sky Survey , the position of the acoustic peak from the cosmic microwave background observations, and large-scale structure formation from the 2dFGRS survey, to put constraints on the parameters of the model. To check the consistency of this action, we compare the age of old cosmological objects with the age of the Universe. In the combined analysis with all the observations, we find the parameters of the model as $R_0 = 6.192^{+0.167}_{-0.177} \times H_0^2$ and $\Omega_m = 0.278^{+0.273}_{-0.278}$.

DOI: 10.1103/PhysRevD.76.044008 PACS numbers: 04.50.+h, 95.36.+x, 98.80.−k

I. INTRODUCTION

Recent observations of supernova type Ia (SNIa) provide the main evidence for the accelerating expansion of the Universe [1,2]. Analysis of SNIa and the cosmic microwave background radiation (CMB) observations indicates that about 70% of the total energy of the Universe is made by the dark energy and the rest of it is in the form of dark matter with a few percent of baryonic matter [3–5]. The "cosmological constant" is a possible explanation of the present dynamics of the Universe [6]. This term in Einstein field equations can be regarded as a fluid with the equation of state of $w = -1$. However, there are two problems with the cosmological constant, namely, the *fine-tuning* and the *cosmic coincidence*. In the framework of quantum field theory, the vacuum expectation value is 123 orders of magnitude larger than the observed value of 10^{-47} GeV^4. The absence of a fundamental mechanism which sets the cosmological constant to zero or to a very small value is the cosmological constant problem. The second problem, known as the cosmic coincidence, asks why the energy densities of dark energy and dark matter are nearly equal today.

There are various solutions for this problem, such as the decaying cosmological constant models. A nondissipative minimally coupled scalar field, the so-called quintessence field, can play the role of this time varying cosmological constant [7–9]. The ratio of the energy density of this field to the matter density in this model increases by the expansion of the Universe, and, after a while, dark energy becomes the dominant term of the energy-momentum tensor. One of the features of this model is the variation of the equation of state during the expansion of the Universe. Various quintessence models, like k-essence [10], tachyonic matter [11], phantom [12,13] and Chaplygin gas [14], provide various equations of state for the dark energy [13,15–21].

Another approach dealing with this problem involves using the modified gravity by changing the Einstein-Hilbert action [22]. Recently, a great deal of attention has been devoted to this era because of the prediction of early and late time accelerations in these models [23]. While it seems that the modified gravity and dark energy models are completely different approaches to explain cosmic acceleration, it is possible to unify them in one formalism [24].

In this work we obtain the dynamics of the modified gravity $f(R) = \sqrt{R^2 - R_0^2}$ in the Palatini formalism [25] and use the cosmological observations such as SNIa, SDSS (Sloan Digital Sky Survey), acoustic peak in CMB, and structure formation to put constraints on the parameter of the action. Our motivation for using the action of $f(R) = \sqrt{R^2 - R_0^2}$ is that for the small Ricci curvatures we will have a minimum value of $R_v = \sqrt{2}R_0$, which provides a late time accelerating expansion of the Universe [26]. Expanding this action in the power series, we get $1/R^n$ terms, where around the vacuum solution the $1/R$ term will be dominated and results are similar to that of the Carroll *et al.* model. In the Palatini formalism, if we add an extra term of R^3/α^2 to the action with $\alpha \gg R_0$, this will unify the inflation and cosmic acceleration by means that we will also have an early time inflation for the Universe with $R_v = \alpha$ [27]. Since we are doing the observational tests at the present time, we can ignore the cubic term in our analysis.

In Sec. II we derive the dynamics of the Hubble parameter and the scale factor in Palatini formalism for the general case of $f(R)$ gravity. In Sec. III, using the action $f(R) = \sqrt{R^2 - R_0^2}$, we obtain the dynamics of the Universe. In Sec. IV we use the observations from the evolution of the background, such as SNIa, CMB, and baryonic acoustic oscillation, to constrain the parameters of the model. Section V studies constraints from the large-scale structure formation, and in Sec. VI we compare the age of the Universe from the model with the age of old cosmological objects. The conclusion is presented in Sec. VII.

II. MODIFIED GRAVITY MODELS IN PALATINI

An alternative approach dealing with the acceleration problem of the Universe involves changing the gravity law through the modification of the action of gravity by using $f(R)$ instead of the Einstein-Hilbert action. For an arbitrary action of gravity, there are two main approaches to extract the field equations. The first one is the so-called metric formalism in which the variation of the action is performed with respect to the metric. In the second approach, Palatini formalism, the connection and metric are considered independent of each other and we have to do variations for those two parameters independently. The general form of the action in Palatini formalism is

$$S[f; g, \hat{\Gamma}, \Psi_m] = -\frac{1}{2\kappa}\int d^4x\sqrt{-g}f(R) + S_m[g_{\mu\nu}, \Psi_m], \tag{1}$$

where $\kappa = 8\pi G$ and $S_m[g_{\mu\nu}, \Psi_m]$ is the matter action which depends only on the metric $g_{\mu\nu}$ and on the matter fields Ψ_m. $R = R(g, \hat{\Gamma}) = g^{\mu\nu}R_{\mu\nu}(\hat{\Gamma})$ is the generalized Ricci scalar and $R_{\mu\nu}$ is the Ricci tensor of the affine connection which is independent of the metric. Varying the action with respect to the metric results in

$$f'(R)R_{\mu\nu}(\hat{\Gamma}) - \tfrac{1}{2}f(R)g_{\mu\nu} = \kappa T_{\mu\nu}, \tag{2}$$

where the prime is the differential with respect to the Ricci scalar and $T_{\mu\nu}$ is the energy-momentum tensor,

$$T_{\mu\nu} = \frac{-2}{\sqrt{-g}}\frac{\delta S_m}{\delta g^{\mu\nu}}. \tag{3}$$

Varying the action with respect to the connection and after contraction gives us the equation that determines the generalized connection as

$$\hat{\nabla}_\alpha[f'(R)\sqrt{-g}g^{\mu\nu}] = 0, \tag{4}$$

where $\hat{\nabla}$ is the covariant derivative with respect to the affine connection. We can see that the connections are the Christoffel symbols of the new metric $h_{\mu\nu}$, where it is conformally related to the original one via $h_{\mu\nu} = f'(R)g_{\mu\nu}$.

Equation (2) shows that, in contrast to the metric variation approach, the field equations are second order in this formalism, and it seems more intuitive to have second order equations instead of fourth order. On the other hand, fourth order differential equations have an instability problem [28]. We use the Friedmann-Robertson-Walker (FRW) metric for the Universe as follows:

$$ds^2 = -dt^2 + a(t)^2\delta_{ij}dx^i dx^j, \tag{5}$$

and assume the Universe is filled with perfect fluid with the energy-momentum tensor of $T^\nu_\mu = \mathrm{diag}(-\rho, p, p, p)$; taking the trace of Eq. (2) gives

$$Rf'(R) - 2f(R) = \kappa T, \tag{6}$$

where $T = g^{\mu\nu}T_{\mu\nu} = -\rho + 3p$. Using the generalized Einstein equation (2) and the FRW metric, we obtain the generalized FRW equation as follows [29]:

$$\left(H + \frac{1}{2}\frac{\dot{f}'}{f'}\right)^2 = \frac{1}{6}\frac{\kappa(\rho + 3p)}{f'} + \frac{1}{6}\frac{f}{f'}. \tag{7}$$

For the cosmic fluid with the equation of state of $p = p(\rho)$, using the continuity equation and the trace of the field equation we can express the time derivative of the Ricci scalar as

$$\dot{R} = 3\kappa H\frac{(1 - 3p')(\rho + p)}{Rf'' - f'(R)}. \tag{8}$$

Using Eq. (6) we obtain the density of matter in terms of the Ricci scalar as

$$\kappa\rho = \frac{2f - Rf'}{1 - 3\omega}, \tag{9}$$

where $w = p/\rho$. Substituting (9) in (7) we obtain the dynamics of the Universe in terms of the Ricci scalar

$$H^2 = \frac{1}{6(1 - 3\omega)f'}\frac{3(1 + \omega)f - (1 + 3\omega)Rf'}{[1 + \frac{3}{2}(1 + \omega)\frac{f''(2f - Rf')}{f'(Rf'' - f')}]^2}. \tag{10}$$

On the other hand, using Eq. (6) and the continuity equation, the scale factor can be obtained in terms of the Ricci scalar

$$a = \left[\frac{1}{\kappa\rho_0(1 - 3\omega)}(2f - Rf')\right]^{-1/3(1+\omega)}, \tag{11}$$

where ρ_0 is the energy density at the present time and we set $a_0 = 1$. Now, for a modified gravity action, omitting the Ricci scalar in favor of the scale factor between Eqs. (10) and (11) we can obtain the dynamics of the Universe [i.e. $H = H(a)$]. For the matter dominant epoch $\omega = 0$, these equations reduce to

$$H^2 = \frac{1}{6f'}\frac{3f - Rf'}{[1 + \frac{3}{2}\frac{f''(2f - Rf')}{f'(Rf'' - f')}]^2}, \tag{12}$$

$$a = \left[\frac{1}{\kappa\rho_0}(2f - Rf')\right]^{-1/3}. \tag{13}$$

III. MODIFIED GRAVITY WITH THE ACTION OF $f(R) = \sqrt{R^2 - R_0^2}$

In this section our aim is to apply the action of $f(R) = \sqrt{R^2 - R_0^2}$ in Eqs. (10) and (11) to obtain the dynamics of the Universe. For simplicity, we use dimensionless parameters in our calculation defined by

$$f(R)=H_0^2\sqrt{X^2-X_0^2} \tag{14}$$

in which H_0 is the Hubble parameter at the present time and $X\equiv\frac{R}{H_0^2}$ and $X_0\equiv\frac{R_0}{H_0^2}$. For convenience, we can write the action and its derivatives as

$$f(R)=H_0^2F(X), \tag{15}$$

$$f'(R)=F'(X), \tag{16}$$

$$f''(R)=\frac{F''(X)}{H_0^2}, \tag{17}$$

where the derivative on the right-hand side of the equations is with respect to X (i.e. $'=\frac{d}{dX}$). We can write (12) with a new parameter X as

$$\mathcal{H}(X)=\frac{1}{6F'}\frac{3F-XF'}{(1+\frac{3}{2}\frac{F''(2F-XF')}{F'(XF''-F')})^2}, \tag{18}$$

where $\mathcal{H}(X)=H^2/H_0^2$ and H_0 is the Hubble parameter at the present time. Using the definition of $\Omega_m(X)\equiv\kappa\rho_m/(3H^2)$ from Eq. (9), we can obtain $\Omega_m(X)$ in terms of X as

$$\Omega_m(X)=\frac{2F-XF'}{3}. \tag{19}$$

We use $\Omega_m(X)=\Omega_m a^{-3}$ (where $\Omega_m\equiv\Omega_m^{(0)}$) and substitute F in terms of X from (14) to obtain the scale factor in terms of X as

$$a=\left[\frac{1}{3\Omega_m}\left(\frac{X^2-2X_0^2}{\sqrt{X^2-X_0^2}}\right)\right]^{-1/3}, \tag{20}$$

where, to have a positive scale factor, X should change in the range of $X\geq\sqrt{2}X_0$. It should be noted that this model has only one free parameter of X_0. X_p represents the value of X at the present time, and from (18) we can find X_p in terms of X_0. On the other hand, substituting $X_p=g(X_0)$ in (19) we will have a direct relation between X_0 and Ω_m. So, knowing X_0 from observation one can also calculate Ω_m.

In the next section we will compare observations with the dynamics provided by this model in the matter dominant epoch. However, we can see how the Universe expands at the radiation dominant epoch. We set $p=1/3\rho$ which implies a traceless energy-momentum tensor, and using our proposed action in Eq. (6), we get a constant Ricci scalar of $R=\sqrt{2}R_0$ for this area. Substituting this constant curvature in Eq. (7) we have

$$H^2=\frac{\kappa}{3\sqrt{2}}\rho-\frac{1}{6\sqrt{2}}R_0. \tag{21}$$

Since R_0 is of the order of H_0^2 (see [26]), for the early Universe we can ignore the second term on the right-hand side of this equation, which results in the scale factor increasing as $a\propto t^{1/2}$.

IV. OBSERVATIONAL CONSTRAINTS FROM THE BACKGROUND EVOLUTION

In this section we compare the new SNIa Gold sample and Supernova Legacy Survey data, the location of the baryonic acoustic oscillation peak from the SDSS, and the location of acoustic peak from the CMB observation to constrain the parameters of the model. We choose various priors applied in this analysis as shown in Table I.

A. Comparing the modified gravity model with supernova type Ia: Gold sample

The supernova type Ia experiments provided the main evidence for the present acceleration of the Universe. Since 1995 two teams from the *High-Z Supernova Search* and the *Supernova Cosmology Project* have discovered several types of Ia supernovas at high redshifts [17,33]. Riess *et al.* (2004) announced the discovery of 16 type Ia supernovas with the Hubble Space Telescope. This new sample includes 6 of the 7 most distant ($z>1.25$) type Ia supernovas. They determined the luminosity distance of these supernovas and, with the previously reported algorithms, obtained a uniform 157 Gold sample of type Ia supernovas [34–36]. Recently, a new data set of the Gold sample with a smaller systematic error containing 156 supernova Ia has been released [37]. In this work we use this data set as the new Gold sample SNIa.

More recently, the SNLS Collaboration released the first year data of its planned five-year Supernova Legacy Survey [38]. An important aspect to be emphasized on the SNLS data is that they seem to be in better agreement with WMAP results than the Gold sample [39].

We calculate the apparent magnitude from the $f(R)$ modified gravity and compare it with the new SNIa Gold sample and the SNLS data set. The supernova measured apparent magnitude m includes reddening, K correction, etc., which here all these effects have been removed. The apparent magnitude is related to the (dimensionless) luminosity distance, D_L, of an object at redshift z through

$$m=\mathcal{M}+5\log D_L(z;X_0), \tag{22}$$

where

TABLE I. Different priors on the parameter space, used in the likelihood analysis.

Parameter	Prior	
$\Omega_{\rm tot}$	1.00	Fixed
$\Omega_b h^2$	0.020 ± 0.005	Top hat (BBN) [30]
h	$\cdots$	Free [31,32]
w	0	Fixed

$$D_L(z; X_0) = (1+z)\int_0^z \frac{dz' H_0}{H(z')}. \tag{23}$$

Also,

$$\mathcal{M} = M + 5\log\left(\frac{c/H_0}{1\ \mathrm{Mpc}}\right) + 25, \tag{24}$$

where M is the absolute magnitude. The distance modulus μ is defined as

$$\mu \equiv m - M = 5\log D_L(z; X_0) + 5\log\left(\frac{c/H_0}{1\ \mathrm{Mpc}}\right) + 25, \tag{25}$$

or

$$\mu = 5\log D_L(z; X_0) + \bar{M}. \tag{26}$$

To compare the theoretical results with the observational data, we calculate the theoretical distance modulus. The distance modulus can be written in terms of the new parameter X as

$$D_L = \frac{1}{3}\frac{(2F - XF')^{1/3}}{(3\Omega_m)^{2/3}}\int_{X_p}^{X}\frac{F' - XF''}{(2F - XF')^{2/3}}\frac{dX}{\mathcal{H}(X)}. \tag{27}$$

To put a constraint on the model parameter, the first step is to compute the quality of the fitting through the least squared fitting quantity χ^2 defined by

$$\chi^2(\bar{M}, X_0) = \sum_i \frac{[\mu_{\mathrm{obs}}(z_i) - \mu_{\mathrm{th}}(z_i; X_0, \bar{M})]^2}{\sigma_i^2}, \tag{28}$$

where σ_i is all of the observational uncertainty in the distance modulus. To constrain the parameters of the model, we use the likelihood statistical analysis

$$\mathcal{L}(\bar{M}, X_0) = \mathcal{N} e^{-\chi^2(\bar{M}, X_0)/2}, \tag{29}$$

where $\mathcal{N}$ is a normalization factor. The parameter $\bar{M}$ is a nuisance parameter and should be marginalized (integrated out) leading to a new $\bar{\chi}^2$ defined as

$$\bar{\chi}^2 = -2\ln\int_{-\infty}^{+\infty} e^{-\chi^2/2} d\bar{M}. \tag{30}$$

Using Eqs. (28) and (30), we find

$$\bar{\chi}^2(X_0) = \chi^2(\bar{M} = 0, X_0) - \frac{B(X_0)^2}{C} + \ln(C/2\pi), \tag{31}$$

where

$$B(X_0) = \sum_i \frac{[\mu_{\mathrm{obs}}(z_i) - \mu_{\mathrm{th}}(z_i; X_0, \bar{M} = 0)]}{\sigma_i^2} \tag{32}$$

and

$$C = \sum_i \frac{1}{\sigma_i^2}. \tag{33}$$

Equivalent to marginalization is the minimization with respect to $\bar{M}$. One can show that $\bar{\chi}^2$ can be expanded in terms of $\bar{M}$ as [40]

$$\chi^2_{\mathrm{SNIa}}(X_0) = \chi^2(\bar{M} = 0, X_0) - 2\bar{M}B + \bar{M}^2 C, \tag{34}$$

which has a minimum for $\bar{M} = B/C$:

$$\chi^2_{\mathrm{SNIa}}(X_0) = \chi^2(\bar{M} = 0, X_0) - \frac{B(X_0)^2}{C}. \tag{35}$$

Using Eq. (35) we can find the best fit values of the model parameters, minimizing $\chi^2_{\mathrm{SNIa}}(X_0)$. Using the new Gold sample SNIa, the best fit values for the free parameter of the model are $X_0 = 6.207^{+0.230}_{-0.147}$ which states $\Omega_m = 0.276^{+0.376}_{-0.240}$, with $\chi^2_{\mathrm{min}}/N_{\mathrm{d.o.f}} = 0.912$ at 1σ level of confidence. The corresponding value for the Hubble parameter at the minimized χ^2 is $h = 0.63$, and since we have already marginalized over this parameter we do not assign an error bar for it. The best fit values for the parameters of the model by using SNLS supernova data are $X_0 = 6.604^{+0.290}_{-0.303}$ which indicates $\Omega_m = 0.233^{+0.483}_{-0.233}$ with $\chi^2_{\mathrm{min}}/N_{\mathrm{d.o.f.}} = 0.86$ at 1σ level of confidence. Figures 1 and 2 show the comparison of the theoretical prediction of the distance modulus by using the best fit value of X_0 and observational values from the new Gold sample and the SNLS supernova Ia, respectively. In Figs. 5 and 6 the relative likelihood for X_0 is indicated. We report the best value of X_0 at 1σ and 2σ confidence levels and other derived parameters in Table II.

B. CMB shift parameter

Before the last scattering, the photons and baryons are tightly coupled by Compton scattering and behave as a fluid. The oscillations of this fluid, occurring as a result of the balance between the gravitational interactions and the

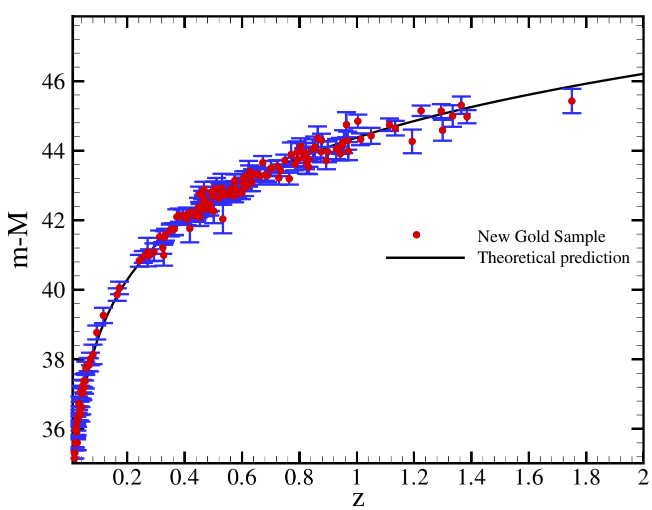

FIG. 1 (color online). Distance modulus of the SNIa new Gold sample in terms of redshift. The solid line shows the best fit values with the corresponding parameters of $h = 0.63$, $\Omega_m = 0.276^{+0.376}_{-0.240}$, $X_0 = 6.207^{+0.230}_{-0.147}$ in the 1σ level of confidence with $\chi^2_{\mathrm{min}}/N_{\mathrm{d.o.f.}} = 0.912$ for the $f(R)$ model.

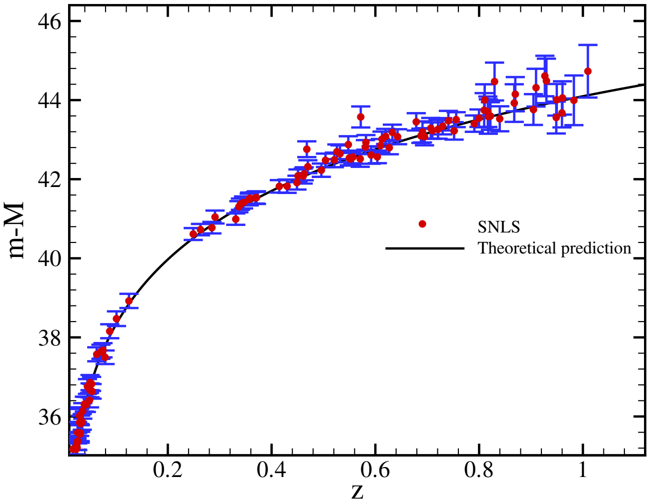

FIG. 2 (color online). Distance modulus of the SNLS supernova data in terms of redshift. The solid line shows the best fit values with the corresponding parameters of $h = 0.70$, $\Omega_m = 0.233^{+0.483}_{-0.233}$, and $X_0 = 6.604^{+0.290}_{-0.303}$ in the 1σ level of confidence with $\chi^2_{\rm min}/N_{\rm d.o.f.} = 0.86$ for the $f(R)$ model.

photon pressure, lead to the familiar spectrum of peaks and troughs in the averaged temperature anisotropy spectrum which we measure today. The odd peaks correspond to maximum compression of the fluid, the even ones to rarefaction [41]. In an idealized model of the fluid, there is an analytic relation for the location of the mth peak: $l_m \approx m l_A$ [42,43], where l_A is the acoustic scale which may be calculated analytically and depends on both pre- and post-recombination physics as well as the geometry of the Universe. The acoustic scale corresponds to the Jeans length of photon-baryon structures at the last scattering surface some $\sim$379 Kyr after the big bang [5]. The apparent angular size of the acoustic peak can be obtained by dividing the comoving size of the sound horizon at the decoupling epoch $r_s(z_{\rm dec})$ by the comoving distance of the observer to the last scattering surface $r(z_{\rm dec})$:

$$\theta_A = \frac{\pi}{l_A} \equiv \frac{r_s(z_{\rm dec})}{r(z_{\rm dec})}. \tag{36}$$

The size of the sound horizon in the numerator of Eq. (36) corresponds to the distance that a perturbation of pressure can travel from the beginning of the Universe up to the last scattering surface and is given by

$$r_s(z_{\rm dec}) = \int_{z_{\rm dec}}^{\infty} \frac{v_s(z')dz'}{H(z')/H_0}, \tag{37}$$

where $v_s(z)^{-2} = 3 + 9/4 \times \rho_b(z)/\rho_{\rm rad}(z)$ is the sound velocity in units of speed of light from the big bang up to the last scattering surface [19,42] and the redshift of the last scattering surface, $z_{\rm dec}$, is given by [42]

$$\begin{aligned} z_{\rm dec} &= 1048[1 + 0.001\,24(\omega_b)^{-0.738}][1 + g_1(\omega_m)^{g_2}], \\ g_1 &= 0.0783(\omega_b)^{-0.238}[1 + 39.5(\omega_b)^{0.763}]^{-1}, \\ g_2 &= 0.560[1 + 21.1(\omega_b)^{1.81}]^{-1}, \end{aligned} \tag{38}$$

where $\omega_m \equiv \Omega_m h^2$ and $\omega_b \equiv \Omega_b h^2$. Changing the parameters of the model can change the size of the apparent acoustic peak and subsequently the position of $l_A \equiv \pi/\theta_A$ in the power spectrum of temperature fluctuations on CMB. The simple relation $l_m \approx m l_A$, however, does not hold very well for the first peak, although it is better for higher peaks [2]. Driving effects from the decay of the gravitational potential as well as contributions from the Doppler shift of the oscillating fluid introduce a shift in the spectrum. A good parametrization for the location of the peaks and troughs is given by [43,44]

$$l_m = l_A(m - \phi_m) \tag{39}$$

where ϕ_m is the phase shift determined predominantly by pre-recombination physics, and is independent of the geometry of the Universe. Instead of the peak locations of the power spectrum of CMB, one can use another model independent parameter, which is the so-called shift parameter $\mathcal{R}$,

$$\mathcal{R} \propto \frac{l_1^{\rm flat}}{l_1} \tag{40}$$

where $l_1^{\rm flat}$ corresponds to the flat pure-CDM model with $\Omega_m = 1.0$ and the same ω_m and ω_b as the original model. The location of the first acoustic peak can be determined in the model by Eq. (39) with $\phi_1(\omega_m, \omega_b) \simeq 0.27$ [43,44]. It is easily shown that the shift parameter is as follows [45]:

$$\mathcal{R} = \sqrt{\Omega_m} \frac{D_L(z_{\rm dec}; X_0)}{(1 + z_{\rm dec})}. \tag{41}$$

In writing the shift parameter in this form we have implicitly assumed that photons follow geodesics determined by the Levi-Civita connection. Furthermore, in order to use the shift parameter, the evolution of the Universe is considered in such a way that at the decoupling we have standard matter dominated behavior. Since we do not have an explicit expression for the Hubble parameters in terms of redshift, it is useful to rewrite the shift parameter in terms of the dimensionless parameter X as follows:

$$\begin{aligned} \mathcal{R} &= \sqrt{\Omega_m H_0^2} \int_0^{z_{\rm dec}} \frac{dz}{H(z)} = \sqrt{\Omega_m H_0^2} \int_{R_{\rm dec}}^{R_p} \frac{a'(R)}{a^2(R)} \frac{dR}{H(R)} \\ &= \frac{\Omega_m^{1/6}}{3^{4/3}} \int_{X_p}^{X_{\rm dec}} \frac{F' - XF''}{(2F - XF')^{2/3}} \frac{dX}{\mathcal{H}(X)}. \end{aligned} \tag{42}$$

The observational results of CMB experiments correspond to a shift parameter of $\mathcal{R} = 1.716 \pm 0.062$ (given by WMAP, CBI, ACBAR) [5,46]. One of the advantages of using the parameter $\mathcal{R}$ is that it is independent of the Hubble constant. In order to put a constraint on the model from CMB, we compare the observed shift parameter with that of the model using likelihood statistics [45]:

$$\mathcal{L} \sim e^{-\chi^2_{\rm CMB}/2} \tag{43}$$

where

$$\chi^2_{\rm CMB} = \frac{[\mathcal{R}_{\rm obs} - \mathcal{R}_{\rm the}]^2}{\sigma^2_{\rm CMB}}. \tag{44}$$

C. Baryon acoustic oscillations

The large-scale correlation function measured from the 46 748 *luminous red galaxies* (LRG) spectroscopic sample of the SDSS includes a clear peak at about 100 Mpc h^{-1} [47]. This peak was identified with the expanding spherical wave of baryonic perturbations originating from acoustic oscillations at recombination. The comoving scale of this shell at recombination is about 150 Mpc in radius. A dimensionless and H_0 independent parameter of this observation is

$$\mathcal{A} = \sqrt{\Omega_m}\left[\frac{H_0 D_L^2(z_{\rm SDSS}; X_0)}{H(z_{\rm SDSS}; X_0) z^2_{\rm SDSS}(1 + z_{\rm SDSS})^2}\right]^{1/3} \tag{45}$$

or

$$\mathcal{A} = \sqrt{\Omega_m}\mathcal{H}(X)^{-1/3}\left[\frac{1}{z_{\rm SDSS}}\int_0^{z_{\rm SDSS}}\frac{dz}{\mathcal{H}(X)}\right]^{2/3}. \tag{46}$$

We can write the above dimensionless quantity in terms of our model parameter as

$$A = \sqrt{\Omega_m}\mathcal{H}(X)^{-1/3}\left[\frac{(3\Omega_m)^{-1/3}}{3z_{\rm SDSS}} \times \int_{X_p}^{X_{\rm SDSS}}\frac{(F' - XF'')dX}{\mathcal{H}(X)(2F - XF')^{2/3}}\right]^{2/3}. \tag{47}$$

We can put the robust constraint on the $f(R)$ modified gravity model using the value of $\mathcal{A} = 0.469 \pm 0.017$ from the LRG observation at $z_{\rm SDSS} = 0.35$ [47]. This observation permits the addition of one more term in the χ^2 of Eqs. (35) and (44) to be minimized with respect to $H(z)$ model parameters. This term is

$$\chi^2_{\rm SDSS} = \frac{[\mathcal{A}_{\rm obs} - \mathcal{A}_{\rm the}]^2}{\sigma^2_{\rm SDSS}}. \tag{48}$$

This is the third observational constraint for our analysis.

D. Combined analysis: SNIa + CMB + SDSS

In this section we combine SNIa data (from the SNIa new Gold sample and SNLS) and CMB data from the WMAP with the recently observed baryonic peak from the SDSS to constrain the parameter of the modified gravity model by minimizing the combined $\chi^2 = \chi^2_{\rm SNIa} + \chi^2_{\rm CMB} + \chi^2_{\rm SDSS}$ [48].

The best values of the model parameters from the fitting with the corresponding error bars from the likelihood function marginalizing over the Hubble parameter in the multidimensional parameter space are $X_0 = 6.169^{+0.170}_{-0.184}$ which corresponds to $\Omega_m = 0.281^{+0.277}_{-0.281}$ at the 1σ confidence level with $\chi^2_{\rm min}/N_{\rm d.o.f.} = 0.902$. The Hubble parameter corresponding to the minimum value of χ^2 is $h = 0.63$. Here we obtain an age of $14.65^{+0.29}_{-0.28}$ Gyr for the Universe. Using the SNLS data, the best fit values of the model parameter are $X_0 = 6.311^{+0.178}_{-0.194}$ which states that $\Omega_m = 0.265^{+0.292}_{-0.265}$ at the 1σ confidence level with $\chi^2_{\rm min}/N_{\rm d.o.f.} = 0.85$. Table II indicates the best fit values for the cosmological parameters with 1σ and 2σ levels of confidence. The relative likelihood analyses for X_0 using CMB and SDSS observations are shown in Figs. 5 and 6.

V. CONSTRAINTS BY LARGE-SCALE STRUCTURE

So far we have only considered observational results related to the background evolution. In this section, using the linear approximation of structure formation, we obtain the growth index of structures and compare it with the result of observations by the 2-degree Field Galaxy Redshift Survey (2dFGRS).

The evolution of structures in the modified gravity has been studied through the spherical collapse and perturbation of the FRW metric. Recently, a procedure has been put forward by Lue, Scoccimarro, and Starkman which relies on the assumption that Birkhoff's theorem holds in the more general setting of modified gravity theories [49]. According to this procedure, it is assumed that the growth of large-scale structure can be modeled in terms of a uniform sphere of dust of constant mass, such that the evolution inside the sphere is determined by the FRW metric. Using Birkhoff's theorem, the spacetime metric in the empty exterior is then taken to be Schwarzschild-like. The components of the exterior metric are then uniquely determined by smoothly matching the interior and exterior regions. In the Palatini formalism the metric outside the spherical distribution of matter depends on the density of matter which may modify the Newtonian limit of these theories [50]. In this case Eq. (49) may change; however, here we assume a Schwarzschild-like Newtonian limit.

The continuity and modified Poisson equations for the density contrast $\delta = \delta\rho/\bar{\rho}$ in the cosmic fluid provide the evolution of the density contrast in the linear approximation (i.e. $\delta \ll 1$) [51,52] as

$$\ddot{\delta} + 2\frac{\dot{a}}{a}\dot{\delta} - [v_s^2\nabla^2 + 4\pi G\rho]\delta = 0, \tag{49}$$

where the dot denotes the derivative with respect to time. The effect of modified gravity in the evolution of the structures in this equation enters through its influence on the expansion rate.

The linear Newtonian approach is valid for the perturbations of the subhorizon scales with $\delta < 1$ [51–53]. For perturbations larger than the Jeans length, $\lambda_J = \pi^{1/2} v_s / \sqrt{G\rho}$, Eq. (49) for cold dark matter (CDM) reduces to

$$\ddot{\delta} + 2\frac{\dot{a}}{a}\dot{\delta} - 4\pi G\rho\delta = 0. \tag{50}$$

The equation for the evolution of the density contrast can be rewritten in terms of the scale factor as

$$\frac{d^2\delta}{da^2} + \frac{d\delta}{da}\left[\frac{\ddot{a}}{\dot{a}^2} + \frac{2H}{\dot{a}}\right] - \frac{3H_0^2}{2\dot{a}^2 a^3}\Omega_m \delta = 0. \tag{51}$$

In order to use the constraint from the large-scale structure we should rewrite the above equation in terms of X. So we have

$$\dot{a} = aH(X), \qquad \ddot{a} = aH^2(X) + a^2 H(X) H'(X)\frac{dX}{da}. \tag{52}$$

Using Eq. (52), Eq. (51) becomes

$$\frac{d^2\delta}{da^2} + \frac{d\delta}{da}\left[\frac{3}{a} + \frac{\mathcal{H}'(X)}{\mathcal{H}(X)}\frac{dX}{da}\right] - \frac{3\Omega_m}{2\mathcal{H}^2(X)a^5}\delta = 0. \tag{53}$$

The numerical solution of Eq. (53) in the FRW universe for the two cases of $f(R)$ gravity and the ΛCDM model with the same matter density content is compared in Fig. 3.

In the linear perturbation theory, the peculiar velocity field $\mathbf{v}$ is determined by the density contrast [51,54] as

$$\mathbf{v}(\mathbf{x}) = H_0 \frac{f}{4\pi}\int \delta(\mathbf{y})\frac{\mathbf{x}-\mathbf{y}}{|\mathbf{x}-\mathbf{y}|^3} d^3\mathbf{y}, \tag{54}$$

where the growth index f is defined by

$$f = \frac{d\ln\delta}{d\ln a}, \tag{55}$$

and it is proportional to the ratio of the second term of Eq. (50) (friction) to the third (Poisson) term.

We use the evolution of the density contrast δ to compute the growth index of structure f, which is an important quantity for the interpretation of peculiar velocities of galaxies [54,55]. Replacing the density contrast with the growth index in Eq. (51) results in the evolution of the growth index as

$$\frac{df}{d\ln a} = \frac{3H_0^2}{2\dot{a}^2 a}\Omega_m - f^2 - f\left[1 + \frac{\ddot{a}}{aH^2}\right]. \tag{56}$$

The above equation in terms of a dimensionless quantity is

$$\frac{df}{d\ln a} = \frac{3\Omega_m}{2a\mathcal{H}^2(X)} - f^2 - f\left[2 + \frac{a\mathcal{H}'(X)}{\mathcal{H}(X)}\frac{dX}{da}\right]. \tag{57}$$

Figure 4 shows the numerical solution of Eq. (57) in terms of redshift. As we expected, increasing X_0 causes decreasing Ω_m from the best fit and a decreasing in the evolution of density contrast versus the scale factor and the growth index in the small redshifts. This behavior is the same as what happens in the ΛCDM model.

To put a constraint on the model using large structure formation, we rely on the observation of 220 000 galaxies with the 2dFGRS experiment which provides the numerical value of the growth index [47]. By measurements of the two-point correlation function, the 2dFGRS team reported the redshift distortion parameter of $\beta = f/b = 0.49 \pm 0.09$ at $z = 0.15$, where b is the bias parameter describing the difference in the distribution of galaxies and their masses. Verde *et al.* (2003) used the bispectrum

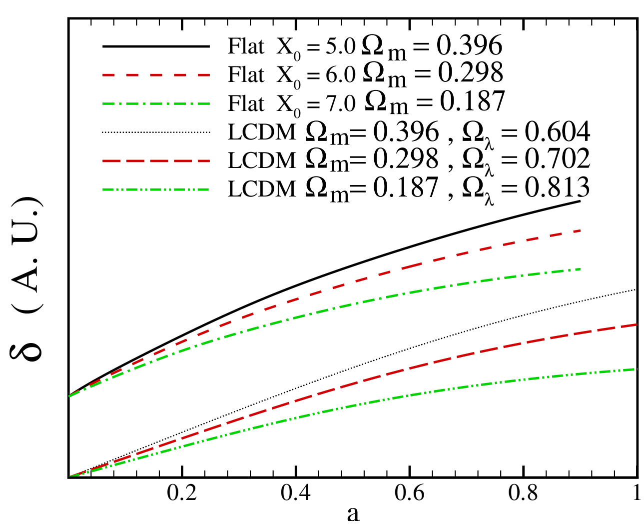

FIG. 3 (color online). Evolution of the density contrast in the $f(R)$ gravity model versus redshift for different values of X_0. For comparison, we plot δ for ΛCDM with the same value of Ω_m. (A.U. stands for an arbitrary unit.)

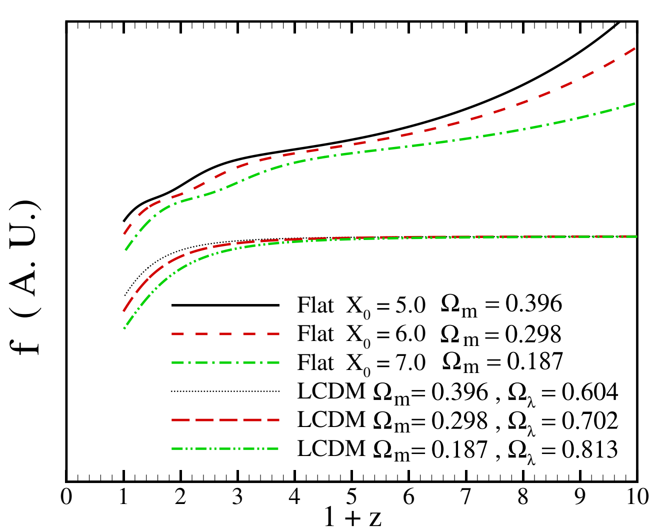

FIG. 4 (color online). Growth index versus redshift for different values of X_0. For comparison we plot f for ΛCDM with the same Ω_m.

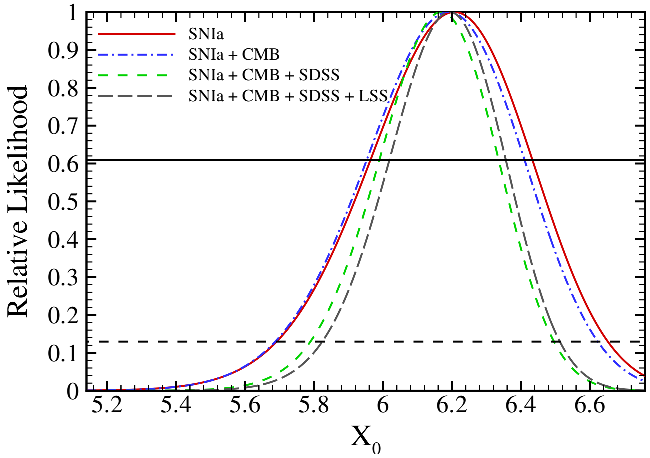

FIG. 5 (color online). Marginalized likelihood functions of the $f(R)$ modified gravity model free parameter, X_0. The solid line corresponds to the likelihood function of fitting the model with SNIa data (new Gold sample), the dash-dot line with the joint SNIa + CMB + SDSS data, and the dashed line corresponds to SNIa + CMB + SDSS + LSS. The intersections of the curves with the horizontal solid and dashed lines give the bounds with 1σ and 2σ levels of confidence, respectively.

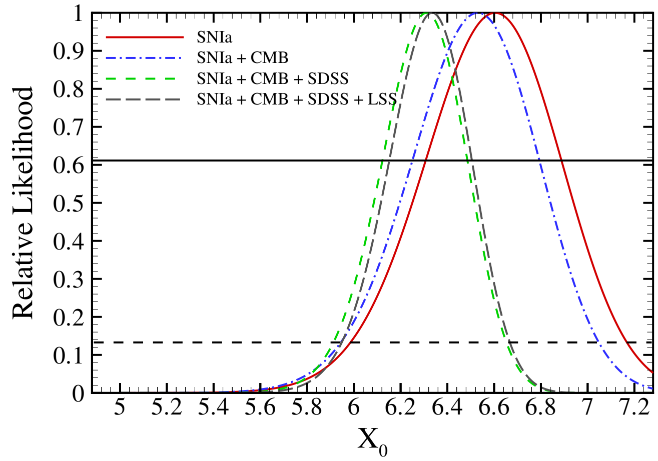

FIG. 6 (color online). Marginalized likelihood functions of the $f(R)$ modified gravity model free parameter, X_0. The solid line corresponds to the likelihood function of fitting the model with SNIa data (SNLS), the dash-dot line with the joint SNIa + CMB + SDSS data, and the dashed line corresponds to SNIa + CMB + SDSS + LSS. The intersections of the curves with the horizontal solid and dashed lines give the bounds with 1σ and 2σ levels of confidence, respectively.

of 2dFGRS galaxies [56,57] and obtained $b_{\rm Verde} = 1.04 \pm 0.11$ which gave $f = 0.51 \pm 0.10$. Now we fit the growth index at the present time derived from Eq. (57) with the observational value. This fitting partially constrains the parameters of the model; however in order to have a better confinement of the parameters, we combine this fitting with those of SNIa + CMB + SDSS which have been discussed in the previous section. We perform the least square fitting by minimizing $\chi^2 = \chi^2_{\rm SNIa} + \chi^2_{\rm CMB} + \chi^2_{\rm SDSS} + \chi^2_{\rm LSS}$, where

$$\chi^2_{\rm LSS} = \frac{[f_{\rm obs}(z = 0.15) - f_{\rm th}(z = 0.15; X_0)]^2}{\sigma^2_{f_{\rm obs}}}. \tag{58}$$

The best fit value with the corresponding error bar for X_0 by using the new Gold sample data is $X_0 = 6.192^{+0.167}_{-0.177}$ which provides $\Omega_m = 0.278^{+0.273}_{-0.278}$ at the 1σ confidence level with $\chi^2_{\rm min}/N_{\rm d.o.f.} = 0.900$. Using the SNLS super-

TABLE II. The best values for the parameters of $f(R)$ modified gravity with the corresponding age for the Universe from fitting with SNIa from the new Gold sample and SNLS data, SNIa + CMB, SNIa + CMB + SDSS, and SNIa + CMB + SDSS + LSS experiments at 1σ and 2σ confidence levels. The value of Ω_m was determined according to Eq. (19).

Observation	X_0	Ω_m	Age (Gyr)
SNIa (new Gold)	$6.207^{+0.230}_{-0.147}$	$0.276^{+0.376}_{-0.240}$	$14.71^{+0.41}_{-0.23}$
	$6.207^{+0.445}_{-0.515}$	$0.276^{+0.727}_{-0.276}$	$14.71^{+0.85}_{-0.75}$
SNIa (new Gold) + CMB	$6.190^{+0.224}_{-0.242}$	$0.278^{+0.365}_{-0.278}$	$14.69^{+0.39}_{-0.37}$
	$6.190^{+0.433}_{-0.503}$	$0.278^{+0.706}_{-0.278}$	$14.69^{+0.82}_{-0.72}$
SNIa (new Gold) + CMB + SDSS	$6.169^{+0.170}_{-0.184}$	$0.281^{+0.277}_{-0.281}$	$14.65^{+0.29}_{-0.28}$
	$6.169^{+0.327}_{-0.380}$	$0.281^{+0.533}_{-0.281}$	$14.65^{+0.58}_{-0.56}$
SNIa (new Gold) + CMB + SDSS + LSS	$6.192^{+0.167}_{-0.177}$	$0.278^{+0.273}_{-0.278}$	$14.69^{+0.29}_{-0.28}$
	$6.192^{+0.321}_{-0.368}$	$0.278^{+0.524}_{-0.278}$	$14.69^{+0.55}_{-0.58}$
SNIa (SNLS)	$6.604^{+0.290}_{-0.303}$	$0.233^{+0.483}_{-0.233}$	$13.91^{+0.61}_{-0.53}$
	$6.604^{+0.562}_{-0.612}$	$0.233^{+0.953}_{-0.233}$	$13.91^{+1.32}_{-0.98}$
SNIa (SNLS) + CMB	$6.530^{+0.269}_{-0.285}$	$0.241^{+0.446}_{-0.241}$	$13.78^{+0.54}_{-0.47}$
	$6.530^{+0.518}_{-0.583}$	$0.241^{+0.860}_{-0.241}$	$13.78^{+1.13}_{-0.89}$
SNIa (SNLS) + CMB + SDSS	$6.311^{+0.178}_{-0.194}$	$0.265^{+0.292}_{-0.265}$	$13.41^{+0.30}_{-0.29}$
	$6.311^{+0.341}_{-0.398}$	$0.265^{+0.560}_{-0.265}$	$13.41^{+0.61}_{-0.57}$
SNIa (SNLS) + CMB + SDSS + LSS	$6.335^{+0.174}_{-0.184}$	$0.263^{+0.286}_{-0.263}$	$13.45^{+0.30}_{-0.28}$
	$6.335^{+0.331}_{-0.386}$	$0.263^{+0.544}_{-0.263}$	$13.45^{+0.59}_{-0.56}$

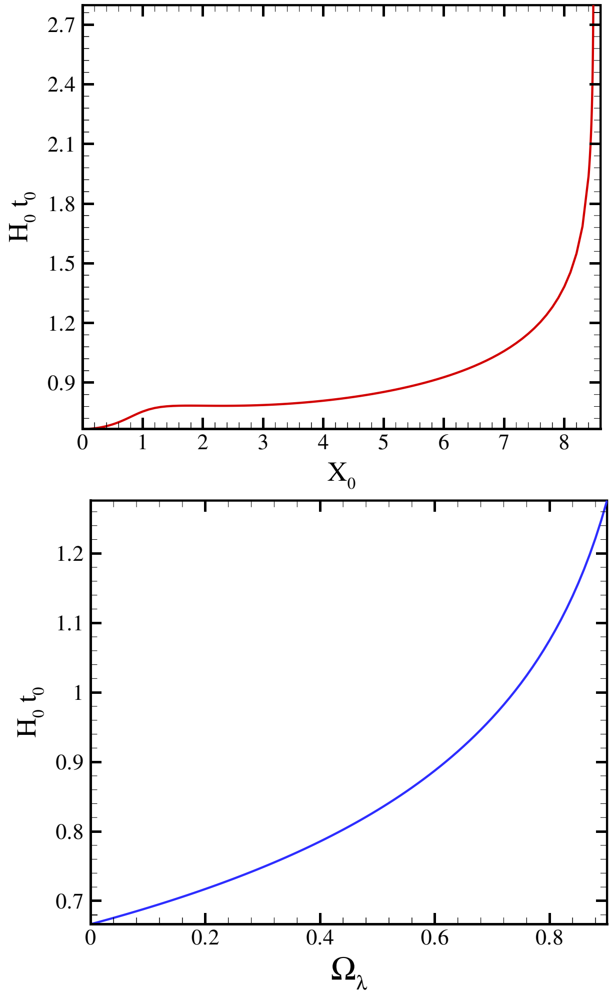

FIG. 7 (color online). $H_0 t_0$ (age of the Universe times the Hubble constant at the present time) as a function of $X_0 = R_0/H_0^2$ (upper panel). $H_0 t_0$ for ΛCDM versus Ω_λ (lower panel). Increasing X_0 gives a longer age for the Universe. This behavior is the same as what happens in ΛCDM.

nova data, the best fit value for the model parameter is $X_0 = 6.335^{+0.174}_{-0.184}$ which gives $\Omega_m = 0.263^{+0.286}_{-0.263}$ at the 1σ confidence level with $\chi^2_{\rm min}/N_{\rm d.o.f.} = 0.86$. The error bars have been obtained through the likelihood functions ($\mathcal{L} \propto e^{-\chi^2/2}$) marginalized over the nuisance parameter h. The likelihood functions for the four cases of (i) fitting the model with supernova data, (ii) a combined analysis with the two experiments of SNIa + CMB, (iii) a combined analysis with the three experiments of SNIa + CMB + SDSS, and (iv) combining all four experiments of SNIa + CMB + SDSS + LSS are shown in Figs. 5 and 6. The best fit value and age of the Universe calculated in the $f(R)$ modified gravity model are reported in Table II.

VI. AGE OF THE UNIVERSE

The age of the Universe integrated from the big bang up to now for a flat universe in terms of X_0 is given by

$$t_0(X_0) = \int_0^{t_0} dt = \int_0^\infty \frac{dz}{(1+z)H(z)} = \frac{1}{3H_0}\int_{X_0}^\infty \frac{F' - XF''}{2F - XF'}\frac{dX}{\mathcal{H}(X)}. \tag{59}$$

Figure 7 shows the dependence of $H_0 t_0$ (the Hubble parameter times the age of the Universe) on X_0 for a flat universe. In the lower panel we show it for ΛCDM for comparison. As we expect, modified gravity behaves as dark energy and increasing X_0 (Ω_λ) results in a longer age for the Universe in the $f(R)$ modified gravity model.

The "age crisis" is one of the main reasons for the acceleration phase of the Universe. The problem is that the Universe's age in the cold dark matter universe is less than the age of old stars in it. Studies on the old stars [58] suggest an age of 13^{+4}_{-2} Gyr for the universe. Richer *et al.* [59] and Hansen *et al.* [60] also proposed an age of 12.7 ± 0.7 Gyr, using the white dwarf cooling sequence method (for a full review of the cosmic age, see [5]). To do another consistency test, we compare the age of the Universe derived from this model with the age of old stars and old high redshift galaxies (OHRG) in various redshifts. Table II shows that the age of the Universe from the combined analysis of SNIa + CMB + SDSS + LSS is $14.69^{+0.29}_{-0.28}$ Gyr and $13.45^{+0.30}_{-0.28}$ Gyr for the new Gold sample and SNLS data, respectively. These values are in agreement with the age of old stars [58]. Here we take three OHRG for comparison with the power-law dark energy model, namely, the LBDS 53W091, a 3.5-Gyr old radio galaxy at $z = 1.55$ [61]; the LBDS 53W069, a 4.0-Gyr old radio galaxy at $z = 1.43$ [62]; and a quasar, APM 08279 + 5255 at $z = 3.91$ with an age of $t = 2.1^{+0.9}_{-0.1}$ Gyr [63]. The latter has, once again, led to the "age crisis." An interesting point about this quasar is that it cannot be accommodated in the ΛCDM model [64]. To quantify the age-consistency test we introduce the expression τ as

$$\tau = \frac{t(z; X_0)}{t_{\rm obs}} = \frac{t(z; X_0)H_0}{t_{\rm obs}H_0}, \tag{60}$$

where $t(z)$ is the age of the Universe, obtained from Eq. (59), and $t_{\rm obs}$ is an estimation for the age of an old cosmological object. In order to have a compatible age for the Universe, we should have $\tau > 1$. Table III reports the value of τ for the three mentioned OHRG with various observations. We see that $f(R)$ modified gravity, with the parameters from the combined observations, provides a compatible age for the Universe, compared to the age of old objects, while the SNLS data result in a shorter age for the Universe. Once again, APM 08279 + 5255 at $z = 3.91$ has a longer age than the Universe but gives better results than most cosmological models [65,66].

TABLE III. The value of τ for three high redshift objects, using the parameters of the model derived from fitting with the observations at 1σ and 2σ levels of confidence.

Observation	LBDS 53W069 $z = 1.43$	LBDS 53W091 $z = 1.55$	APM 0.8279 + 5255 $z = 3.91$
SNIa (new Gold)	$1.23^{+0.05}_{-0.03}$	$1.32^{+0.05}_{-0.03}$	$0.86^{+0.37}_{-0.05}$
	$1.23^{+0.10}_{-0.09}$	$1.32^{+0.11}_{-0.10}$	$0.86^{+0.38}_{-0.08}$
SNIa (new Gold) + CMB	$1.23^{+0.05}_{-0.04}$	$1.32^{+0.05}_{-0.05}$	$0.86^{+0.37}_{-0.06}$
	$1.23^{+0.10}_{-0.08}$	$1.32^{+0.11}_{-0.09}$	$0.86^{+0.38}_{-0.09}$
SNIa (new Gold) + CMB + SDSS	$1.23^{+0.03}_{-0.04}$	$1.32^{+0.04}_{-0.04}$	$0.85^{+0.36}_{-0.05}$
	$1.23^{+0.07}_{-0.06}$	$1.32^{+0.08}_{-0.07}$	$0.85^{+0.37}_{-0.07}$
SNIa (new Gold) + CMB + SDSS + LSS	$1.23^{+0.04}_{-0.03}$	$1.32^{+0.04}_{-0.04}$	$0.86^{+0.36}_{-0.05}$
	$1.23^{+0.07}_{-0.06}$	$1.32^{+0.08}_{-0.08}$	$0.86^{+0.37}_{-0.07}$
SNIa (SNLS)	$1.19^{+0.08}_{-0.08}$	$1.28^{+0.08}_{-0.07}$	$0.84^{+0.37}_{-0.07}$
	$1.19^{+0.17}_{-0.12}$	$1.28^{+0.19}_{-0.13}$	$0.84^{+0.39}_{-0.11}$
SNIa (SNLS) + CMB	$1.17^{+0.07}_{-0.06}$	$1.26^{+0.07}_{-0.06}$	$0.83^{+0.36}_{-0.06}$
	$1.17^{+0.14}_{-0.11}$	$1.26^{+0.16}_{-0.12}$	$0.83^{+0.38}_{-0.10}$
SNIa (SNLS) + CMB + SDSS	$1.13^{+0.04}_{-0.04}$	$1.21^{+0.04}_{-0.04}$	$0.79^{+0.34}_{-0.05}$
	$1.13^{+0.07}_{-0.07}$	$1.21^{+0.08}_{-0.07}$	$0.79^{+0.34}_{-0.07}$
SNIa (SNLS) + CMB + SDSS + LSS	$1.13^{+0.04}_{-0.03}$	$1.22^{+0.04}_{-0.04}$	$0.79^{+0.34}_{-0.05}$
	$1.13^{+0.08}_{-0.06}$	$1.22^{+0.08}_{-0.07}$	$0.79^{+0.35}_{-0.07}$

VII. CONCLUSION

Here, in this work, we obtained the dynamics of the Universe with $f(R) = \sqrt{R^2 - R_0^2}$ gravity in the Palatini formalism and compared it with the recent cosmological observations. Expanding this function in a power series can cover $1/R^n$ models of modified gravity. Also, adding a cubic term as R^3/α^2 where $\alpha \gg R_0$ can produce an inflationary epoch at the early Universe.

The comparison of the model has been performed with the supernova type Ia Gold sample and SNLS supernova data, the CMB shift parameter, the location of the baryonic acoustic oscillation peak observed by SDSS, and large-scale structure formation data by 2dFGRS. The best parameters obtained from fitting with the new Gold sample data are $h = 0.63$, $X_0 = 6.192^{+0.167}_{-0.177}$ which provides $\Omega_m = 0.278^{+0.273}_{-0.278}$ at the 1σ confidence level with $\chi^2_{\rm min}/N_{\rm d.o.f.} = 0.900$. Using the SNLS supernova data, the best fit value for the model parameter is $X_0 = 6.335^{+0.174}_{-0.184}$ which gives $\Omega_m = 0.263^{+0.286}_{-0.263}$ at the 1σ confidence level with $\chi^2_{\rm min}/N_{\rm d.o.f.} = 0.85$. We get almost the same amount of matter density as the ΛCDM model and the other dark energy models. Here the extra term of action R_0 plays the role of the cosmological constant. By the expansion of this action in power series, we can replace the parameter of model R_0 with that of μ in $f(R) = R - \mu^4/R$ as $R_0 = \sqrt{2}\mu^2$. Recent cosmological tests of $1/R$ provide almost the same number for μ that we have obtained in this work [67].

We also performed the age test, comparing the age of old stars and old high redshift galaxies with the age derived from this model. From the best fit parameters of the model using the new Gold sample and SNLS, we obtained an age of $14.69^{+0.29}_{-0.28}$ Gyr and $13.45^{+0.30}_{-0.20}$ Gyr, respectively, for the Universe, which is in agreement with the age of old stars. We also chose two high redshift radio galaxies at $z = 1.55$ and $z = 1.43$ with a quasar at $z = 3.91$. The ages of the first two objects are consistent with the age of the Universe, which means that they are younger than the Universe, while the third one is not.

ACKNOWLEDGMENTS

We would like to thank the anonymous referee for his useful comments on this work.

[1] A. G. Riess *et al.*, Astron. J. **116**, 1009 (1998).
[2] S. Perlmutter *et al.*, Astrophys. J. **517**, 565 (1999).
[3] C. L. Bennett *et al.*, Astrophys. J. Suppl. Ser. **148**, 1 (2003).
[4] H. V. Peiris *et al.*, Astrophys. J. Suppl. Ser. **148**, 213 (2003).
[5] D. N. Spergel, L. Verde, H. V. Peiris *et al.*, Astrophys. J. **148**, 175 (2003).
[6] S. Weinberg, Rev. Mod. Phys. **61**, 1 (1989); S. M. Carroll, Living Rev. Relativity **4**, 1 (2001); P. J. E. Peebles and B. Ratra, Rev. Mod. Phys. **75**, 559 (2003); T. Padmanabhan, Phys. Rep. **380**, 235 (2003).

[7] C. Wetterich, Nucl. Phys. **B302**, 668 (1988); P. J. E. Peebles and B. Ratra, Astrophys. J. **325**, L17 (1988); B. Ratra and P. J. E. Peebles, Phys. Rev. D **37**, 3406 (1988); J. A. Frieman, C. T. Hill, A. Stebbins, and I. Waga, Phys. Rev. Lett. **75**, 2077 (1995); M. S. Turner and M. White, Phys. Rev. D **56**, R4439 (1997); R. R. Caldwell, R. Dave, and P. J. Steinhardt, Phys. Rev. Lett. **80**, 1582 (1998); A. R. Liddle and R. J. Scherrer, Phys. Rev. D **59**, 023509 (1998); I. Zlatev, L. Wang, and P. J. Steinhardt, Phys. Rev. Lett. **82**, 896 (1999); P. J. Steinhardt, L. Wang, and I. Zlatev, Phys. Rev. D **59**, 123504 (1999); D. F. Torres, Phys. Rev. D **66**, 043522 (2002).

[8] L. Amendola, Phys. Rev. D **62**, 043511 (2000); L. Amendola and D. Tocchini-Valentini, Phys. Rev. D **64**, 043509 (2001); **66**, 043528 (2002); L. Amendola, Mon. Not. R. Astron. Soc. **342**, 221 (2003); M. Pietroni, Phys. Rev. D **67**, 103523 (2003); D. Comelli, M. Pietroni, and A. Riotto, Phys. Lett. B **571**, 115 (2003); U. Franca and R. Rosenfeld, Phys. Rev. D **69**, 063517 (2004); X. Zhang, Phys. Lett. B **611**, 1 (2005).

[9] P. J. E. Peebles and R. Ratra, Astrophys. J. **325**, L17 (1988).

[10] C. Armendariz-Picon, V. Mukhanov, and P. J. Steinhardt, Phys. Rev. Lett. **85**, 4438 (2000).

[11] J. S. Bagla, H. K. Jassal, and T. Padmanabhan, Phys. Rev. D **67**, 063504 (2003).

[12] R. R. Caldwell, Phys. Lett. B **545**, 23 (2002).

[13] R. R. Caldwell, M. Kamionkowski, and N. N. Weinberg, Phys. Rev. Lett. **91**, 071301 (2003).

[14] A. Kamenshchik, U. Moschella, and V. Pasquier, Phys. Lett. B **511**, 265 (2001).

[15] S. Arbabi Bidgoli, M. S. Movahed, and S. Rahvar, Int. J. Mod. Phys. D **15**, 1455 (2006).

[16] L. Wang, R. R. Caldwell, J. P. Ostriker, and P. J. Steinhardt, Astrophys. J. **530**, 17 (2000).

[17] S. Perlmutter, M. S. Turner, and M. White, Phys. Rev. Lett. **83**, 670 (1999).

[18] L. Page *et al.*, Astrophys. J. Suppl. Ser. **148**, 233 (2003).

[19] M. Doran, M. Lilley, J. Schwindt, and C. Wetterich, Astrophys. J. **559**, 501 (2001).

[20] M. Doran and M. Lilley, Mon. Not. R. Astron. Soc. **330**, 965 (2002).

[21] R. R. Caldwell and M. Doran, Phys. Rev. D **69**, 103517 (2004).

[22] S. M. Carroll, V. Duvvuri, M. Trodden, and M. S. Turner, Phys. Rev. D **70**, 043528 (2004).

[23] S. Nojiri and S. D. Odintsov, Gen. Relativ. Gravit. **36**, 1765 (2004); M. E. Soussa and R. P. Woodard, Gen. Relativ. Gravit. **36**, 855 (2004); G. Allemandi, A. Borowiec, and M. Francaviglia, Phys. Rev. D **70**, 103503 (2004); D. A. Easson, Int. J. Mod. Phys. A **19**, 5343 (2004); S. M. Carroll, A. De Felice, V. Duvvuri, D. A. Easson, M. Trodden, and M. S. Turner, Phys. Rev. D **71**, 063513 (2005); S. Carloni, P. K. S. Dunsby, S. Capozziello, and A. Troisi, Classical Quantum Gravity **22**, 4839 (2005); S. Capozziello, V. F. Cardone, and A. Troisi, Phys. Rev. D **71**, 043503 (2005); G. Cognola, E. Elizalde, S. Nojiri, S. D. Odintsov, and S. Zerbini, J. Cosmol. Astropart. Phys. 02 (2005) 010; S. Nojiri, S. D. Odintsov, and S. Tsujikawa, Phys. Rev. D **71**, 063004 (2005); T. Clifton and J. D. Barrow, Phys. Rev. D **72**, 103005 (2005); S. Das, N. Banerjee, and N. Dadhich, Classical Quantum Gravity **23**, 4159 (2006); S. Capozziello, V. F. Cardone, E. Elizalde, S. Nojiri, and S. D. Odintsov, Phys. Rev. D **73**, 043512 (2006); T. P. Sotiriou, Classical Quantum Gravity **23**, 5117 (2006); A. De Felice, M. Hindmarsh, and M. Trodden, J. Cosmol. Astropart. Phys. 08 (2006) 005; S. Nojiri and S. D. Odintsov, Phys. Rev. D **74**, 086005 (2006); A. F. Zakharov, A. A. Nucita, F. De Paolis, and G. Ingrosso, Phys. Rev. D **74**, 107101 (2006); P. Zhang, Phys. Rev. D **73**, 123504 (2006); K. Atazadeh and H. R. Sepangi, Int. J. Mod. Phys. D **16**, 687 (2007); S. M. Carroll, I. Sawicki, A. Silvestri, and M. Trodden, New J. Phys. **8**, 323 (2006); D. Huterer and E. V. Linder, Phys. Rev. D **75**, 023519 (2007); X. h. Jin, D. j. Liu, and X. z. Li, arXiv:astro-ph/0610854; N. J. Poplawski, arXiv:gr-qc/0610133; V. Faraoni, Phys. Rev. D **74**, 104017 (2006); Y. S. Song, W. Hu, and I. Sawicki, Phys. Rev. D **75**, 044004 (2007); I. Navarro and K. Van Acoleyen, arXiv:gr-qc/061112; R. Bean, D. Bernat, L. Pogosian, A. Silvestri, and M. Trodden, Phys. Rev. D **75**, 064020 (2007); T. Chiba, T. L. Smith, and A. L. Erickcek, Phys. Rev. D **75**, 124014 (2007); V. Faraoni and S. Nadeau, Phys. Rev. D **75**, 023501 (2007); E. O. Kahya and V. K. Onemli, arXiv:gr-qc/0612026.

[24] S. Rahvar and Y. Sobouti, arXiv:0704.0680.

[25] D. N. Vollick, Phys. Rev. D **68**, 063510 (2003).

[26] S. Baghram, M. Farhang, and S. Rahvar, Phys. Rev. D **75**, 044024 (2007).

[27] T. P. Sotiriou, Phys. Rev. D **73**, 063515 (2006).

[28] V. V. Nesterenko, Phys. Rev. D **75**, 087703 (2007).

[29] G. Allemandi, A. Borowiec, and M. Francaviglia, Phys. Rev. D **70**, 043524 (2004); **70**, 103503 (2004); M. Amarzguioui, O. Elgaroy, D. F. Mota, and T. Multamaki, Astron. Astrophys. **454**, 707 (2006); T. P. Sotiriou and S. Liberati, Ann. Phys. (N.Y.) **322**, 935 (2007).

[30] A. Melchiorri, L. Mersini, C. L. Ödman, and M. Trodden, arXiv:astro-ph/0211522.

[31] W. L. Freedman *et al.*, Astrophys. J. Lett. **553**, 47 (2001).

[32] X. Zhang and F. Q. Wu, Phys. Rev. D **72**, 043524 (2005).

[33] B. P. Schmidt *et al.*, Astrophys. J. **507**, 46 (1998).

[34] A. G. Riess *et al.*, Astrophys. J. **607**, 665 (2004).

[35] J. L. Tonry *et al.*, Astrophys. J. **594**, 1 (2003).

[36] B. J. Barris *et al.*, Astrophys. J. **602**, 571 (2004).

[37] The Gold data set is available at http://braeburn.pha.jhu.edu/ariess/R06.

[38] P. Astier *et al.*, Astron. Astrophys. **447**, 31 (2006).

[39] H. K. Jassal *et al.*, arXiv:astro-ph/0601389.

[40] S. Nesseris and L. Perivolaropoulos, Phys. Rev. D **70**, 043531 (2004).

[41] W. Hu, N. Sugiyama, and J. Silk, Nature (London) **386**, 37 (1997).

[42] W. Hu and N. Sugiyama, Astrophys. J. **444**, 489 (1995).

[43] W. Hu, M. Fukugita, M. Zaldarriaga, and M. Tegmark, Astrophys. J. **549**, 669 (2001).

[44] M. Doran and M. Lilley, Mon. Not. R. Astron. Soc. **330**, 965 (2002).

[45] J. R. Bond, G. Efstathiou, and M. Tegmark, Mon. Not. R. Astron. Soc. **291**, L33 (1997); A. Melchiorri, L. Mersini, C. J. Odman, and M. Trodden, Phys. Rev. D **68**, 043509 (2003); C. J. Odman, A. Melchiorri, M. P. Hobson, and A. N. Lasenby, Phys. Rev. D **67**, 083511 (2003).

[46] T. J. Pearson *et al.* (CBI Collaboration), Astrophys. J. **591**, 556 (2003); C. L. Kuo *et al.* (ACBAR Collaboration), Astrophys. J. **600**, 32 (2004).

[47] D. J. Eisenstein *et al.*, Astrophys. J. **633**, 560 (2005).

[48] C. L. Bennett, R. S. Hill, and G. Hinshaw, Astrophys. J. Suppl. Ser. **148**, 97 (2003).

[49] A. Lue, R. Scoccimarro, and G. Starkman, Phys. Rev. D **69**, 044005 (2004).

[50] G. J. Olmo, Phys. Rev. Lett. **95**, 261102 (2005); G. J. Olmo, Phys. Rev. Lett. **98**, 061101 (2007).

[51] T. Padmanabhan, *Structure Formation in the Universe* (Cambridge University Press, Cambridge, England, 1993).

[52] R. H. Brandenberger, in *The Early Universe and Observational Cosmology*, edited by N. Breton, J. L. Cervantes-Cota, and M. Salgado, Lecture Notes in Physics Vol. 646 (Springer, Berlin/Heidelberg, 2004), p. 127.

[53] K. Koyama and R. Maartens, J. Cosmol. Astropart. Phys. 01 (2006) 016.

[54] P. J. E. Peebles, *The Large Scale Structure of the Universe* (Princeton University Press, Princeton, NJ, 1980).

[55] R. Mansouri and S. Rahvar, Int. J. Mod. Phys. D **11**, 321 (2002).

[56] L. Verde, M. Kamionkowski, J. J. Mohr, and A. J. Benson, Mon. Not. R. Astron. Soc. **321**, L7 (2001).

[57] O. Lahav, S. L. Bridle, and W. J. Percival (2dFGRS Team), Mon. Not. R. Astron. Soc. **333**, 961 (2002).

[58] E. Carretta *et al.*, Astrophys. J. **533**, 215 (2000); B. Chaboyer and L. M. Krauss, Astrophys. J. Lett. **567**, L45 (2002).

[59] H. B. Richer *et al.*, Astrophys. J. **574**, L151 (2002).

[60] B. M. S. Hansen *et al.*, Astrophys. J. **574**, L155 (2002).

[61] J. Dunlop *et al.*, Nature (London) **381**, 581 (1996); H. Spinrard, Astrophys. J. **484**, 581 (1997).

[62] J. Dunlop, in *The Most Distant Radio Galaxies*, edited by H. J. A. Rottgering, P. Best, and M. D. Lehnert (Kluwer, Dordrecht, 1999), p. 71.

[63] G. Hasinger, N. Schartel, and S. Komossa, Astrophys. J. Lett. **573**, L77 (2002).

[64] D. Jain and A. Dev, Phys. Lett. B **633**, 436 (2006).

[65] M. Sadegh Movahed and S. Rahvar, Phys. Rev. D **73**, 083518 (2006).

[66] S. Rahvar and M. Sadegh Movahed, Phys. Rev. D **75**, 023512 (2007).

[67] N. J. Poplawski, Classical Quantum Gravity **24**, 3013 (2007).